Characterization of the *Helicobacter pylori* NikR−P_{ureA} DNA Interaction: Metal Ion Requirements and Sequence Specificity†

Nuvjeevan S. Dosanjh, Nicole A. Hammerbacher, and Sarah L. J. Michel*

Department of Pharmaceutical Sciences, School of Pharmacy, University of Maryland, Baltimore, Maryland 21201-1180

Received October 6, 2006; Revised Manuscript Received December 13, 2006

ABSTRACT: *HP*NikR, a prokaryotic nickel binding transcription factor, is found in *Helicobacter pylori* where it functions as a regulator of multiple genes, including those involved in acid adaptation and nickel ion homeostasis. Particularly important is *HP*NikR's role in the regulation of the nickel-dependent enzyme urease which is critical for the organism's survival in the acidic environment of the gastric epithelium. The target operator sequences of the genes regulated by *HP*NikR do not contain any identifiable palindromes, and the exact mechanism(s) of the *HP*NikR−DNA recognition event is unknown. *HP*NikR was expressed and purified as a soluble protein containing mixed α/β secondary structure with evidence of a tertiary fold. A direct and competitive fluorescence anisotropy (FA) assay to probe both the metal ion requirements and sequence specificity of *HP*NikR for P_{ureA}, the operator sequence for the urease gene, was developed. FA studies revealed that apo-*HP*NikR did not bind to P_{ureA} while Ni(II)*HP*NikR bound P_{ureA} with nanomolar affinity, but only in the presence of a second metal ion [magnesium, calcium, or manganese(II)], suggesting that *HP*NikR contains a second, low-affinity metal binding site. Cu(II)-*HP*NikR also exhibited a requirement for a second metal ion to accomplish P_{ureA} binding. Removal of a loosely conserved "putative" palindrome sequence in the P_{ureA} operator abrogated *HP*NikR binding. Together, these results support a model of *HP*NikR−P_{ureA} binding in which specific metal ions must be coordinated to high- and low-affinity sites to modulate binding.

Helicobacter pylori is a virulent bacterium that colonizes the highly acidic, mucus layer (or gastric epithelium) of the human stomach, causing gastritis and in some cases gastric cancer (*1*−*4*). More than half of the world's population is infected with *H. pylori*, making it a significant public health threat, and there is a documented need for the development of novel anti-*Helicobacter* agents (*5*). *H. pylori* are among a select number of bacteria that are able to survive in the highly acidic environment of the gastric epithelium: the pH of the gastric epithelium ranges from 4 to 6.5 with periodic acid shocks of pH <2 (*6*, *7*). One of the features that enables *H. pylori* to survive under such conditions is that it releases large quantities of ammonia to neutralize its immediate environment. A key protein involved in *H. pylori* ammonia production is urease, a nickel-dependent enzyme found in very high concentrations (∼10% of total protein content) (*8*−*10*). As well as contending with an acidic environment, *H. pylori* is also exposed to high levels of metal ions which are released from ingested foods at low pH (*11*, *12*). *H. pylori* has evolved sophisticated mechanisms for incorporating and using these metal ions for a number of functions, and one important protein involved in this response is the metalloregulatory protein NikR (*HP*NikR). *HP*NikR is a pleiotropic regulator of multiple genes involved in *H. pylori*'s acid adaptation (*13*).

First identified in *Escherichia coli*, NikR belongs to a family of nickel-dependent regulatory proteins found in both Gram-negative and Gram-positive bacteria (*14*). In *E. coli*, NikR (*EC*NikR) functions as a "sensor" of nickel ions by repressing the transcription of *nik* genes which encode a nickel importer (NikABCDE) (*15*, *16*). In response to high levels of nickel ions, *EC*NikR recognizes a specific palindromic operator sequence, GTATGA-N_{16}-TCATAC, located on the promoter region of the *nikR* gene (*15*). *EC*NikR contains two domains, a C-terminal metal binding domain and an N-terminal DNA binding, domain and is functional as a tetramer, with the C-terminal domain forming a central tetrameric core flanked by two dimeric DNA binding domains (*15*, *17*, *18*). The DNA binding domain adopts a ribbon−helix−helix fold which is a common fold for prokaryotic transcription factors, and the metal binding domain adopts a $\beta\alpha\beta\beta\alpha\beta$ fold (*19*). Nickel(II) coordination at the metal binding domain is mediated by Cys107, His99, and His101 from one of the monomers and His88 from a second monomer [amino acid ligands described with *HP*-NikR numbering (*20*)], and it exhibits a square planar coordination geometry (*19*). Intriguingly, XAS studies have shown that upon DNA binding, the nickel site undergoes a change in coordination geometry, suggesting a communication link between the C-terminal metal binding domains and the N-terminal DNA binding domains (*21*). Studies using gel shift and DNAse footprinting assays revealed that a tighter binding interaction between *EC*NikR and *nikR* (DNA) is achieved when excess nickel is present, leading to the

† We are grateful to the University of Maryland Baltimore for support of this research.

* To whom correspondence should be addressed. Phone: (410) 706-7038. Fax: (410) 706-5017. E-mail: smichel@rx.umaryland.edu.

10.1021/bi062092w CCC: $37.00
Published on Web 02/10/2007

hypothesis that *EC*NikR contains a second, "low-affinity" nickel binding site (*18*, *22*). A recently determined X-ray structure of *EC*NikR bound to *nikR* DNA confirmed this second metal binding site but showed potassium rather than nickel in this site and retention of a square planar coordination geometry at the "high-affinity" nickel binding site (*23*).

*HP*NikR shares significant homology (30% identical and 68% homologous) with *EC*NikR, is also functional as a tetramer, and also binds nickel via Cys107, His99, and His101 from one monomer and His88 from another (*14*, *20*, *24*, *25*). However, unlike *EC*NikR which functions as a transcriptional *represssor* of a single gene (*nikR*), *HP*NikR functions as both a *repressor* and an *activator* of a large and diverse group of genes (*13*). The genes include genes involved in nickel metabolism (e.g., *nixA* and *hpn*), genes involved in iron uptake and storage (e.g., *pfr*, *fur*, and *exbB/exbD*), genes involved in motility (e.g., *cheV*, *flaA*, and *flab*), genes involved in stress response (e.g., *hrcA-grpE-dnaK*), genes encoding outer membrane proteins (e.g., *omp11*, *omp31*, and *omp32*), and genes that encode the urease enzyme (*ureA-ureB*). The genome of *H. pylori* is one quarter of the size of the *E. coli* genome (*26*), and van Vliet et al. (*25*) have suggested that *H. pylori* has evolved to encode proteins, such as *HP*NikR, that act as global regulators of gene transcription.

The evidence for the regulation by *HP*NikR of the genes described above comes primarily from in vivo transcriptome studies (*13*), and for many of these genes, it is not yet known if the observed regulation is a result of direct transcriptional control regulated by *HP*NikR or occurs via an accessory pathway. Recently, a small subset of these genes was studied in more detail in vitro using DNAse footprinting assays. From these studies, seven genes that are directly regulated by *HP*NikR were identified: *UreA* which encodes urease (*27*−*29*), *NixA* which encodes a high-affinity nickel transporter (*29*), *ExbB* which is part of the TonB−ExbBD complex which provides energy for iron or nickel uptake (*28*), *Fur* which encodes the ferric uptake regulator (*28*), *FecA3* and *FrpB4* which are outer-membrane proteins (OMPs) of unknown function (*30*), and *NikR* which encodes NikR (*27*, *28*). *HP*NikR activates *ureA* transcription and represses the other six genes. The recognition sequences of these genes differ, although a putative palindrome required for recognition has been proposed, TATtATT-N_{11}-AATAA-TA (*28*). This recognition sequence is completely different from that identified for *EC*NikR in both sequence and length, suggesting that *HP*NikR may recognize DNA in a manner different from that of *EC*NikR. The ability of *HP*NikR to directly recognize multiple genes raises the question, how does *HP*NikR distinguish between the genes it controls? Our hypothesis is that the specific DNA sequence coupled with the metal ion occupancy of *HP*NikR drives the recognition events. To address this question, we sought to develop a real-time, solution-based assay that would allow us to systematically screen for operator sequences directly recognized by *HP*NikR, quantify the affinity of NikR for these operators, and identify the sequence elements involved in DNA binding. We have developed both a direct and a competitive fluorescence anisotropy (FA)[1] assay that allows us to rapidly screen for such interactions between *HP*NikR and various genes. In this work, we describe the application of this assay in studying the interaction between *HP*NikR and the *ureA* gene promoter which encodes urease and present evidence that *HP*NikR requires a second metal ion for DNA binding.

EXPERIMENTAL PROCEDURES

Cloning and Expression of HPNikR. PCR primers were designed to amplify the *nikR* gene from genomic HP26995 (ATCC, Manassas, VA) with *Nco*I and *Bam*HI restriction sites incorporated. The fragment containing the *nikR* gene was ligated into a pET15b vector (Novagen) that had been cut with the same enzymes such that the protein would be expressed without any affinity tags. The identity of the cloned gene was confirmed by DNA sequencing (University of Maryland Baltimore Biopolymer Facility). When the sequence was confirmed, the pET15b construct containing *H. pylori* NikR was transformed into *E. coli* BL21(DE3) cells (1 L for large-scale expression) and grown in LB medium containing 100 μg/mL ampicillin. Typically, cell cultures were grown for 4 h post-induction with 0.45 mM IPTG before being harvested by centrifugation (7800*g* for 15 min at 4 °C). The cell pellets that were obtained were resuspended in a 20 mM NaH_2PO_4, 500 mM NaCl, 10 mM imidazole buffer (pH 7.5) to which one EDTA-free protease inhibitor tablet was added (Roche) to prevent protease activity. Following lysis with a French press at 1250 psi using a Thermo Spectronic French pressure cell at 4 °C, the cell debris was removed by centrifugation (12100*g* for 15 min at 4 °C).

Purification of *HP*NikR was carried out following the procedures described for the purification of *EC*NikR, with slight modifications (*15*). Because *HP*NikR is a putative nickel binding protein, nickel affinity chromatography was the first type of chromatography that was utilized. Initially, $NiSO_4$ was added to the cytoplasmic extract containing *HP*NikR before the extract was loaded onto the affinity column; however, we later observed that this precaution was unnecessary. A recently published purification of *HP*NikR confirmed our observation (*27*). Purification of the protein was carried out using a pre-equilibrated [with 20 mM NaH_2PO_4, 500 mM NaCl, 10 mM imidazole buffer (pH 7.5)] nickel-loaded 5 mL Hitrap-HP (Amersham) affinity column using an AKTA FPLC system. *HP*NikR was eluted by the application of a linear gradient containing 300 mM imidazole and isolated at ∼150 mM imidazole. The eluted *HP*NikR was then dialyzed against 20 mM Tris and 100 mM NaCl (pH 8.0) in preparation for further purification using anion exchange chromatography. Purification was carried out using a Hitrap Q Sepharose (Amersham) column, pre-equilibrated with 20 mM Tris and 100 mM NaCl (pH 8.0). *HP*NikR was eluted with the application of a linear gradient of NaCl from 100 to 500 mM. The protein typically eluted at a NaCl concentration of ∼200−300 mM and was found to be >95%

[1] Abbreviations: CD, circular dichroism; DEPC, diethyl pyrocarbonate; DTT, dithiothreitol; *EC*, *Escherichia coli*; EDTA, ethylenediaminetetraacetic acid; FA, fluorescence anisotropy; F_{bound}, fraction bound; F, fluorescein; FPLC, fast protein liquid chromatography; HEPES, 4-(2-hydroxyethyl)-1-piperazineethanesulfonic acid; HP, *Helicobacter pylori*; IPTG, isopropyl β-D-thiogalactopyranoside; K_d, dissociation constant; LB, Luria-Bertani; MALDI-TOF, matrix-assisted laser desorption ionization time-of-flight (mass spectrometry); MES, 2-(*N*-morpholino)ethanesulfonic acid; PCR, polymerase chain reaction; *r*, anisotropy; SDS−PAGE, sodium dodecyl sulfate−polyacrylamide gel electrophoresis; Tris, tris(hydroxymethyl)aminomethane.

pure by SDS−PAGE. MALDI-MS was used to confirm the molecular weight (expected, 17 147.2; observed, 17 147.2). Approximately 30−40 mg of *HP*NikR is obtained from a starting culture of 1 L. Because *HP*NikR has several cysteine residues, all further manipulations were carried out anaerobically using a Coy inert atmospheric chamber (95% N_2 and 5% H_2).

Generation of Apo-HPNIKR. Apo-*HP*NikR was prepared by incubation of the protein with 50 mM EDTA and 10 mM DTT overnight at 35 °C followed by exhaustive dialysis with 20 mM Hepes, 100 mM NaCl Chelex-treated buffer (pH 7.5). The dialyzed protein was then buffer exchanged and concentrated using a Centricon-plus 20 device (Millipore) against a Chelex-prepared 20 mM Hepes, 100 mM NaCl, 20 mM glycine buffer (pH 7.5).

Intrinsic Tryptophan Fluorescence Studies. Emission spectra were recorded on an ISS PC1 photon counting spectrofluorometer configured in the L format. The spectra were recorded at 25 °C with excitation at 280 nm, and fluorescence was monitored from 300 to 450 nm. A slit width of 2 nm was used on the excitation and emission monochromaters. Spectra were acquired with 3 μM *HP*NikR protein samples in 20 mM Hepes and 100 mM NaCl (pH 7.5) using a 1 cm path length Spectrosil far-UV quartz window fluorescence cuvette (Starna Cells).

Circular Dichroism (CD) Studies. The secondary structure contents of the apo and holo forms of *HP*NikR were determined by analyzing far-UV CD spectra acquired on a Jasco-810 spectropolarimeter. CD spectra were recorded from 180 to 250 nm at a scan rate of 20 nm/min, with each spectrum representing the average of 10 accumulations. Data were acquired at 25 °C with a 1 mm path length cell with *HP*NikR samples in 20 mM sodium phosphate (pH 7.5). Estimates of secondary structure composition were calculated using the CDPro package, using a 43-protein reference set (*31*). Thermal denaturation studies were recorded with 10 μM protein samples with a 1 mm path length cell. Unfolding was monitored at 222 nm over a temperature range of 5−100 °C.

Metal Binding Titrations. Metal binding titrations were performed in either Teflon-stoppered or screw-capped quartz cuvettes using a Perkin-Elmer Lambda 25 UV−vis spectrometer. Titrations were carried out in 20 mM Hepes, 100 mM NaCl, and 20 mM glycine (pH 7.5) using metal-free reagents and water that had been purified using a MilliQ purification system and passed over Sigma Chelex resin. Upon their preparation, buffers were purged with helium to degas and transferred into a Coy inert atmospheric chamber. The following metal salts or stocks, which were stored anaerobically, were used for the titrations: nickel(II) sulfate hexahydrate (99.99% Ni) from Puratrem and cupric(II) sulfate pentahydrate (98%) from Fisher. Titrations were carried out in triplicate. The binding interaction between apo-*HP*NikR and nickel or copper was assessed spectrophotometrically by the titration of a solution of apo-*HP*NikR (typically 50 μM in 1 mL of buffer) with Ni(II) or Cu(II).

Oligonucleotide Probes. The following HPLC-purified oligonucleotides were purchased from Operon either labeled with fluorescein (F) or unlabeled: (1) P_{ureA}-*F* (49mer), 5′-CTTCAAGATATAACACTAATT[F]CATTTTAAATAATAATTAGTTAATGAA-3′; (2) P_{ureA}-*49* (49mer), 5′-CTTCAAGATATAACACTAATTCATTTTAAATAATAATTAGTTAATGAA-3′; and (3) P_{ureA}-*pal* (without palindromes), 5′-CTTCAAAGATAccccccccAATTCATTTTAccccccccATTAGTTAATGAA-3′. When they were received, the oligonucleotides were resuspended in DNase-free water and quantified. For annealing, each oligonucleotide was mixed such that there was a 1.25:1 ratio of unlabeled to labeled oligonucleotide, in 10 mM Tris, 10 mM NaCl annealing buffer (pH 8.0). The annealing reaction mixtures were placed in a water bath set to a temperature 10 °C greater than the melting temperatures (T_m's) of the component oligonucleotides. The water bath was then immediately turned off, and the annealing reaction mixtures were allowed to cool overnight. Double-stranded oligonucleotides were quantified and stored at −20 °C.

Fluorescence Anisotropy Titrations. A fluorescence anisotropy (FA) assay was developed to study the binding of *HP*NikR to DNA. Measurements were taken with an ISS PC-1 spectrofluorometer configured in the L format. Initially, a full excitation and emission spectrum was run to determine the optimum excitation and emission wavelengths for the experiment. The excitation wavelength and band-pass used in the experiments were 495 and 2 nm, respectively, and the emission wavelength and band-pass were 519 and 1 nm, respectively.

Screening Experiments. To screen for *HP*NikR−DNA binding, a 10 nM solution of fluorescently labeled DNA (P_{ureA}-*F*) in 20 mM HEPES, 100 mM NaCl, and 20 mM glycine (pH 7.5) was added to a 0.5 cm PL Spectrosil far-UV quartz window fluorescence cuvette (Starna Cells) that had been pretreated with a solution of 175 Bloom porcine gelatin (Sigma) to prevent adherence of either the protein or DNA to the cuvette walls (*32*). The gelatin pretreatment was accomplished by heating 1 mL of a 20 mg/mL solution of 175 Bloom porcine gelatin to 55 °C followed by cooling to room temperature. Approximately 8 μL of this solution was then added to the 20 mM HEPES, 100 mM NaCl, 20 mM glycine buffer (pH 7.5) and the mixture stirred continuously overnight. The appropriate double-stranded DNA oligonucleotide was then added to the solution to make up the final 500 μL cuvette volume used for the anisotropy studies. The anisotropy, *r*, of the free DNA oligonucleotide was measured. Apo-*HP*NikR was then titrated into the cuvette from a stock solution [20 mM HEPES, 100 mM NaCl, and 20 mM glycine (pH 7.5)] in a stepwise fashion and the effect on anisotropy recorded. Ni(II) and then Mg(II) or Mg(II) and then Ni(II) were then added, sequentially, and the effect of anisotropy was recorded.

M-HPNikR−P_{ureA}-F Binding Studies. Forward Titrations [M = Ni(II) or Cu(II)]. The anisotropy of fluorescently labeled DNA (P_{UreA}-*F*) in 20 mM HEPES, 100 mM NaCl, 20 mM glycine, 3 mM $MgCl_2$ (or $CaCl_2$ or $MnCl_2$) (pH 7.5) in a 0.5 cm PL Spectrosil far-UV quartz window fluorescence cuvette (Starna Cells) was recorded. M-*HP*NikR [M = Ni(II) or Cu(II)] was then titrated into the cuvette from a stock solution [in 20 mM HEPES, 100 mM NaCl, 20 mM glycine, and 3 mM $MgCl_2$ (or $CaCl_2$ or $MnCl_2$) (pH 7.5)], and the change in anisotropy was recorded. The protein was added until the anisotropy values reached a plateau which indicated saturation. The data were analyzed by converting the anisotropy, *r*, to the fraction bound, F_{bound} (the fraction of M-*HP*NikR bound to DNA at a given DNA concentration), using the equation (*33*):

$$F_{\text{bound}} = \frac{r - r_{\text{free}}}{(r_{\text{bound}} - r)Q + (r - r_{\text{free}})}$$

where r_{free} is the anisotropy of the fluorescein-labeled oligonucleotide, r_{bound} is the anisotropy of the DNA−protein complex at saturation, and Q is the quantum yield ratio of the bound to free form and is calculated from the fluorescence intensity changes that occur ($Q = I_{\text{bound}}/I_{\text{free}}$). Typically, Q values of 0.45 were observed with the exception of experiments involving Mn, where Q values of approximately 0.3 were attained. F_{bound} was plotted against the protein concentration, treating *HP*NikR as a tetramer, and fit using a one-site binding model:

$$\text{P} + \text{D} \rightleftharpoons \text{PD}$$

$$K_{\text{d}} = \frac{[\text{P}][\text{D}]}{[\text{PD}]}$$

$$F_{\text{bound}} = \frac{P_{\text{total}} + D_{\text{total}} + K_{\text{d}} - \sqrt{(P_{\text{total}} + D_{\text{total}} + K_{\text{d}})^2 - 4P_{\text{total}}D_{\text{total}}}}{2D_{\text{total}}}$$

where P is the protein (*HP*NikR) concentration and D is the DNA concentration. Each data point from the fluorescence anisotropy assay represents the average of 31 readings taken over a time course of 100 s. Each titration was carried out in triplicate.

Competitive Anisotropy Titrations. The competitive anisotropy assays were conducted in 20 mM HEPES, 100 mM NaCl, 20 mM glycine, and 3 mM $MgCl_2$ (pH 7.5). In a typical experiment, an unlabeled DNA molecule was titrated into a solution containing 375 nM Ni-*HP*NikR (tetramer) and 15 nM P_{ureA}-*F*, and the decrease in anisotropy (r) as the unlabeled DNA oligomer competed with the labeled oligonucleotide was recorded. The anisotropy was converted to the fraction bound, to take into account changes in quantum yield, using the equation described above. Binding isotherms were fit using Mathematica (version 5.2, Wolfram Research) to a model that involved the mass action equations for the three competing equilibria:

$$\text{P} + \text{D}_{\text{f}} \underset{K_1}{\rightleftharpoons} \text{PD}_{\text{f}} \quad (1)$$

$$\text{P} + \text{D} \underset{K_2}{\rightleftharpoons} \text{PD} \quad (2)$$

$$\text{PD}_{\text{f}} + \text{D} \underset{K_3}{\rightleftharpoons} \text{PD} + \text{D}_{\text{f}} \quad (3)$$

where P is the nickel-bound protein (*HP*NikR), D_f is fluorescently labeled DNA, and D represents unlabeled DNA. The value for K_1 was determined from the forward titrations and thus used as a known parameter for the fit. Mathematica was used to combine eqs 1−3 and to solve the resulting cubic equation in terms of PD_f using nonlinear, least-squares analysis. All titrations were carried out in triplicate.

Electrophoretic Mobility Shift Assay (EMSA). An EMSA between *HP*NikR and DNA was run using a 7% nondenaturing acrylamide gel and a TAE (Tris-acetate EDTA) running buffer containing 800 μM $NiSO_4$ and 3 mM $MgCl_2$. Approximately 250 nM P_{ureA} DNA was incubated with increasing concentrations of Ni-*HP*NikR (250 nM, 1 μM, 5 μM, and 20 μM) for 1 h at room temperature followed by electrophoresis at 4 °C and 100 V. The acrylamide gel was stained with ethidium bromide and viewed with a UV light box.

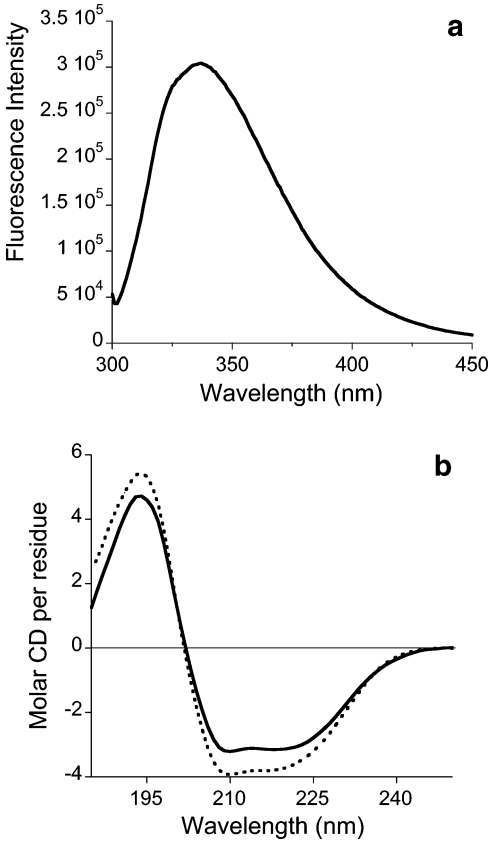

FIGURE 1: (a) Intrinsic tryptophan fluorescence emission spectrum of apo-*HP*NikR (3 μM *HP*NikR monomer in 20 mM Hepes and 100 mM NaCl at pH 7.5 and 25 °C). The protein was excited at 280 nm. (b) CD spectra of 10 μM Ni-*HP*NikR (- - -) and 10 μM apo-*HP*NikR (—) in 25 mM NaH_2PO_4 and 100 mM NaCl at pH 7.5 and 25 °C. The *Y*-axis units are molar CD per residue ($\Delta\epsilon$ in M^{-1} cm^{-1}).

RESULTS

Preparation and Characterization of HPNikR. The gene for *HP*NikR was cloned into a pET-15b vector with no purification tags, overexpressed, and purified by nickel affinity and anion exchange chromatographies using slight modifications of previously reported protocols (*15*, *17*, *20*, *27*−*29*, *34*). The identity of the protein was confirmed by MALDI-MS and the purity by SDS−PAGE. Apo-*HP*NikR was prepared by the anaerobic incubation of the purified protein with 50 mM EDTA and 10 mM DTT followed by extensive dialysis. To confirm that the protein was folded, intrinsic tryptophan fluorescence studies were carried out (Figure 1a). Apo-*HP*NikR exhibited an emission maximum of 338 nm which suggests that the tryptophan residue (W54) resides in a solvent-buried conformation (*33*). There was little perturbation in the fluorescence emission maximum of *HP*NikR in the presence of nickel, suggesting that nickel does not affect the overall fold of the protein (data not shown). Representative far-UV circular dichroism spectra are shown in Figure 1b for both the apo and nickel-bound forms of *HP*NikR. The shape of the spectrum indicates that apo-*HP*NikR contains ordered secondary structure with nickel

binding inducing a small shift in the spectrum. Estimates of secondary structure content using CDPro (*31*) revealed that apo-*HP*NikR is composed of 33% helix, 18% sheet, 21% turn, and 28% unstructured regions and Ni-*HP*NikR contains 40% helix, 14% sheet, 20% turn, and 26% unstructured regions. The results suggest that nickel induces a relatively small conformational change in the protein's overall secondary structure with a slight increase in helical content observed. However, nickel binding does not appear to confer any further structural stability as determined when comparing the CD thermal denaturation profiles of the apoprotein and the Ni-*HP*NikR protein (Figure S1 of the Supporting Information). The helical content estimated by CD for Ni-*HP*NikR compares favorably with that recently calculated from the Ni-*HP*NikR crystal structure (43% helix) (*20*), whereas the sheet content (32%) is an underestimate; it must be noted, however, that there exists a level of uncertainty when predicting β-sheet content particularly in a mixed α/β-containing protein due to the high intensity of the helix spectrum (*35*).

Metal Binding Titrations with Ni(II) and Cu(II). To confirm that apo-*HP*NikR as isolated in our laboratory bound nickel, Ni(II) was added to the protein and the UV−visible spectrum recorded. Upon the addition of 1 equiv of nickel, bands at 304 and 475 nm appeared (Figure S2). The band at 304 nm is likely a charge-transfer band, while the band at 475 nm is a d−d absorbance band (*15*, *34*). The spectrum strongly resembles that of nickel-bound *EC*NikR, and a recently published spectrum of nickel-bound *HP*NikR, and is suggestive of square planar coordination geometry (*15*, *17*, *27*, *34*). To determine the stoichiometry of the interaction between apo-*HP*NikR and nickel, apo-*HP*NikR was titrated with Ni(II). The bands at 304 and 475 nm saturated upon the addition of approximately 1 equiv of nickel which is similar to the observation of Zamble and co-workers where saturation at 0.9 equiv was observed (Figure S3) (*27*). Binding of Cu(II) to apo-HPNikR was carried out analogously. Cu(II)-*HP*NikR exhibited a new band with a maximum around 385 nm which closely matches one reported for Cu-*EC*NikR and a recently published Cu-*HP*NikR spectrum (*27*, *34*) (Figure S4). The band saturated upon the addition of 1 equiv of copper (Figure S5).

Fluorescence Anisotropy Titrations. A fluorescence anisotropy (FA) assay was developed to quantify the interactions between *HP*NikR and DNA. This type of assay has been successfully used to study DNA binding of other prokaryotic metallotranscription factors, including CmtR (*36*), MntR (*37*), and Fur (*38*). An advantage of the FA assay over a traditional electrophoretic gel shift assay (EMSA) or a DNase footprinting study is that it is solution-based and can be used to rapidly screen for a number of different parameters. For the studies described here, a DNA sequence that corresponds to the *ureA* promoter (P_{ureA}) was utilized. *UreA* encodes one of the subunits of urease required for normal *H. pylori* function and is directly regulated by *HP*NikR (*27*−*29*, *39*, *40*). DNase footprinting assays for identifying the region of the *ureA* promoter protected by *HP*NikR have been reported by several research groups (refs *27*−*29* and personnal communication of P. Chivers). Each group has reported a slightly different "protected" sequence; therefore, a DNA molecule that included all of the sequence elements identified by these labs was used for the FA studies. This sequence, named P_{ureA}-*F*, was made up of a single-stranded DNA molecule with a CTTCAAAGATATAA-CACTAAT**T**<u>**F**</u>CATTTAAATAATAATTAGTTAATGAA sequence in which a fluorescein molecule (<u>**F**</u>) was conjugated to a central thymine (bold and underlined) annealed to a complementary, unlabeled strand of DNA. This thymine is located in the linker region between the two proposed palindromes, making it unlikely that fluorescein conjugation at this position will interfere with *HP*NikR−DNA binding.

Magnesium Requirement for Binding. Initial FA titrations were carried out in 20 mM HEPES, 100 mM NaCl, and 20 mM glycine (pH 7.5) which are typical conditions used for FA and are designed to mimic physiological conditions (*36*, *41*, *42*). The addition of up to 4 μM apo-*HP*NikR or 4 μM Ni-*HP*NikR to a 10 nM solution of P_{ureA}-*F* failed to elicit any changes in anisotropy, indicating that DNA binding was not occurring. Surprisingly, the addition of 3 mM magnesium chloride to the P_{ureA}-*F*/Ni-*HP*NikR solution resulted in a significant change in anisotropy, implying that the two macromolecules were binding and suggesting that magnesium plays a crucial role in the Ni-*HP*NikR−P_{ureA} binding event. To examine the relationship between magnesium and nickel in *HP*NikR−P_{ureA} binding in more detail, screening experiments were carried out (Figure 2a,b). In the first experiment, apo-*HP*NikR was titrated into P_{ureA}-*F* under Mg-free buffer conditions [20 mM HEPES, 100 mM NaCl, and 20 mM glycine (pH 7.4)]. The addition of up to 92 equiv of [apo-*HP*NikR]$_4$ failed to result in any changes in anisotropy. The addition of excess Ni(II) to the solution (up to 50 equiv of Ni per apo-*HP*NikR) also did not result in any anisotropy changes. However, the addition of 3 mM $MgCl_2$ to the solution resulted in a large change in anisotropy (Figure 2a), indicative of a binding event. The reverse experiment was also carried out. Here, apo-*HP*NikR was titrated into P_{ureA}-*F* under Mg-free buffer conditions [20 mM HEPES, 100 mM NaCl, and 20 mM glycine (pH 7.4)] followed by addition of up to 3 mM $MgCl_2$. No change in anisotropy was observed. The addition of 4 equiv of Ni(II) (per [apo-*HP*NikR]$_4$) resulted in a large change in anisotropy (Figure 2b) that mirrored the change seen in the first experiment after addition of Mg (Figure 2a). Further addition of Ni(II) did not result in any changes in anisotropy, indicating that only stoichiometric nickel is required for binding. These experiments demonstrate that *HP*NikR requires both nickel and magnesium to bind to P_{ureA} and that nickel likely binds to a high-affinity site due to the requirement of only stoichiometric quantities of nickel for binding, while the affinity of *HP*NikR for magnesium is likely lower due to a requirement of excess magnesium for binding.

To quantify the interaction (K_d) between Ni-*HP*NikR and P_{ureA} in the presence of magnesium, a full FA titration was carried out. In this experiment, Ni-*HP*NikR was titrated into a solution of 15 nM P_{ureA}-*F* that contained 3 mM $MgCl_2$ in the buffer (Figure 3a). The data were fit to a 1:1 binding equilibrium using nonlinear least-squares analysis (treating Ni-*HP*NikR as a tetramer), yielding a dissociation constant, K_d, of $5.7 \pm 0.21 \times 10^{-8}$ M.

Competitive Binding Titration Using Unlabeled UreA. To verify that the fluorophore on P_{ureA}-*F* was not significantly affecting DNA binding, a competitive binding titration was developed. In this assay, *HP*NikR was first titrated with P_{ureA}-*F* followed by addition of an unlabeled DNA molecule

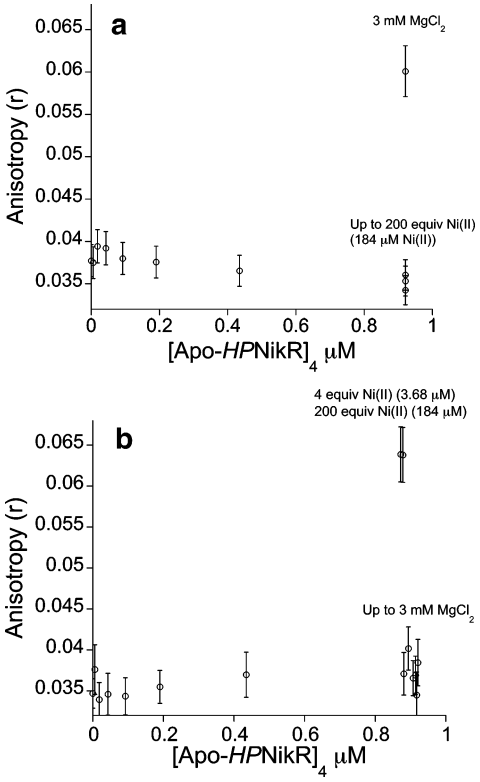

FIGURE 2: Fluorescence anisotropy-monitored binding of *HP*NikR to the ureA promoter. (a) Change in anisotropy, *r*, as apo-*HP*NikR is titrated into P_{ureA}-*F* followed by addition of $NiSO_4$ and then $MgCl_2$. (b) Change in anisotropy, *r*, as apo-*HP*NikR is titrated into P_{ureA}-*F* follwed by addition of $MgCl_2$ and then $NiSO_4$. All FA experiments were performed in 20 mM Hepes, 100 mM NaCl, and 20 mM glycine (pH 7.5) at 25 °C.

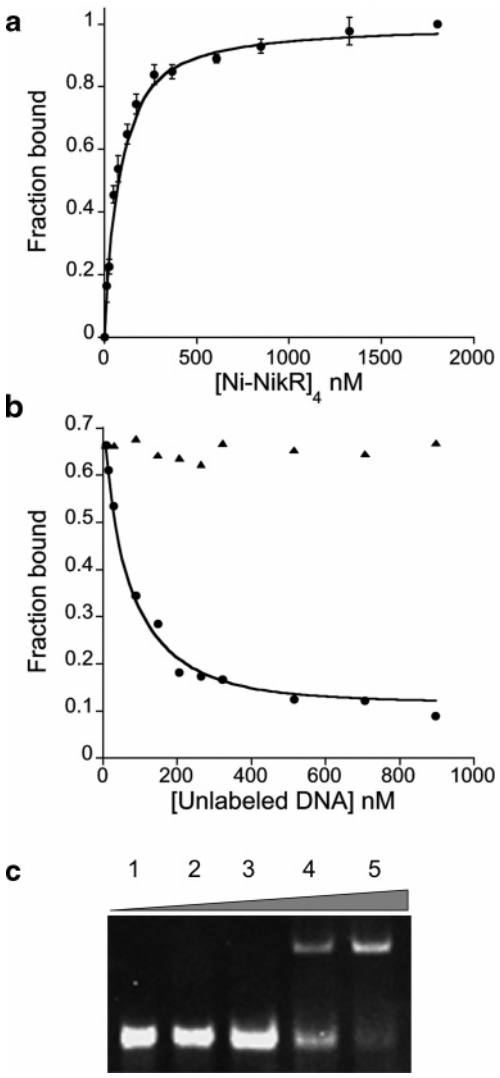

FIGURE 3: DNA binding of Ni-*HP*NikR to the P_{ureA} promoter (P_{ureA}). (a) Change in anisotropy (as fraction bound) upon addition of Ni-*HP*NikR to P_{ureA}-*F*. An average of three sets of binding data is shown, and the solid line represents a nonlinear least-squares fit of the data to a 1:1 binding model. A dissociation constant, K_d, of $5.7 \pm 0.21 \times 10^{-8}$ M was determined. (b) Competitive titration of unlabeled P_{ureA} (49mer) into 15 nM P_{ureA}-*F* and 375 nM NikR (●) and of a palindrome-less P_{ureA} sequence, P_{ureA}-*pal*, into 15 nM P_{ureA}-*F* and 375 nM NikR (▲). Data were fit to a competitive binding equilibrium, and a dissociation constant, K_d, of $(6.7 \pm 0.1) \times 10^{-8}$ M was determined. All FA experiments were performed in 20 mM Hepes, 100 mM NaCl, 20 mM glycine, and 3 mM $MgCl_2$ at pH 7.5 and 25 °C. (c) EMSA between P_{ureA}-*49* and Ni-*HP*NikR in a 7% nondenaturing acrylamide gel and TAE (Tris-acetate EDTA) running buffer with 800 μM $NiSO_4$ and 3 mM $MgCl_2$: lane 1, 250 nM P_{ureA}-*49* alone; lane 2, 250 nM P_{ureA}-*49* with 250 nM Ni-NikR; lane 3, 250 nM P_{ureA}-*49* with 1 μM Ni-NikR; lane 4, 250 nM P_{ureA}-*49* with 5 μM Ni-NikR; and lane 5, 250 nM P_{ureA}-*49* with 20 μM Ni-NikR.

of the same sequence, P_{ureA}-*49* (Table 1). Addition of P_{ureA}-*49* resulted in a decrease in anisotropy, suggesting displacement of P_{ureA}-*F* by P_{ureA}-*49* (Figure 3b). The data were fit to a competitive binding model, and a K_d for P_{ureA} binding of $6.7 \pm 0.10 \times 10^{-8}$ M was determined. This value is very close to the value obtained from the forward titration, suggesting that the fluorophore on P_{ureA}-*F* does not significantly influence DNA binding.

Electrophoretic Mobility Shift Assay. To independently confirm that Ni-*HP*NikR binds to the P_{ureA} sequence, an electrophoretic mobility shift assay (EMSA) was performed (Figure 3c). In this assay, P_{ureA} was incubated with varying amounts of Ni-*HP*NikR in both the presence and absence of 3 mM $MgCl_2$. A gel shift was observed upon addition of 5 μM Ni-*HP*NikR to 250 nM P_{ureA} only in the presence of 3 mM $MgCl_2$, demonstrating that Ni-*HP*NikR binds to the P_{ureA} sequence only when $MgCl_2$ is present and confirming the results of the FA titrations.

Competitive Titrations with a Palindrome-less ureA Sequence. A region of the P_{ureA} sequence made up of the bases TAACACT-X_{11}-AATAATA has been proposed to make up a palindromic recognition sequence (*28*). To test whether this part of the P_{ureA} sequence is required for Ni-*HP*NikR binding and to ascertain whether the binding event between Ni-*HP*NikR and P_{ureA} observed for the FA titrations is specific, a competitive titration with the sequence P_{ureA}-*pal* (5′-CTTCAAAGATAccccccccAATTCATTTTAccccccccA-TTAGTTAATGAA-3′) which does not contain the proposed palindrome was performed. This sequence was not able to compete with the P_{ureA}-*F* sequence, as shown in Figure 3b, indicating that the putative palindrome is required for Ni-*HP*NikR−P_{ureA} binding.

Magnesium Titrations. Experiments to determine the amount of magnesium required for a Ni-*HP*NikR−P_{ureA} binding were performed (Figure 4). Magnesium was titrated into a solution of the Ni-*HP*NikR−P_{ureA}-*F* complex (4 μM and 15 nM, respectively) and the change in anisotropy monitored. An initial anisotropy change was observed upon

Table 1: Oligonucleotides Used in This Study[a]

P_{ureA}-F	CTTCAAAGATATAACACTAATTCATTTTAAATAATAATTAGTTAATGAA
P_{ureA}-49	CTTCAAAGATATAACACTAATTCATTTTAAATAATAATTAGTTAATGAA
P_{ureA}-pal	CTTCAAAGATACCCCCCCAATTCATTTTACCCCCCCATTAGTTAATGAA

[a] The putative palindrome is boxed. For P_{ureA}-*F*, the fluorescently labeled thymine is highlighted with a black background.

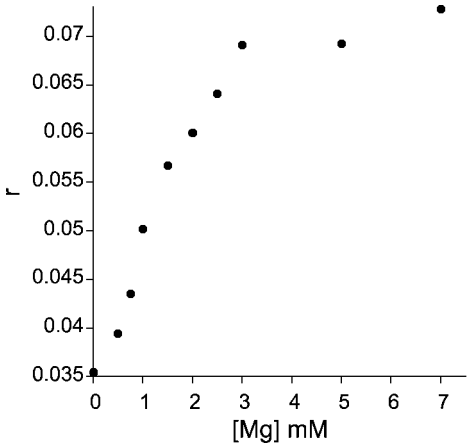

FIGURE 4: Plot of the change in anisotropy (*r*) as a Ni-*HP*NikR/P_{ureA} solution (4 μM monomer) is titrated with $MgCl_2$ (20 mM Hepes, 100 mM NaCl, and 20 mM glycine at 25 °C).

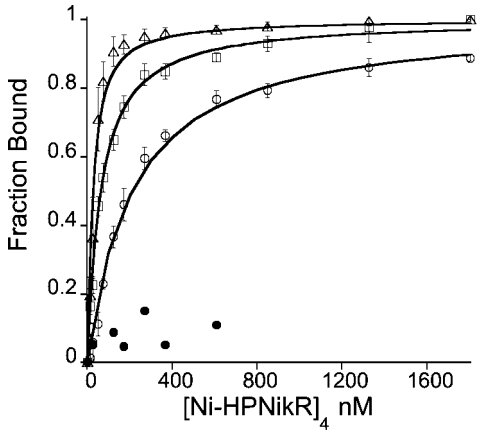

FIGURE 5: Comparison of the change in anisotropy (as fraction bound) upon addition of Ni-*HP*NikR to P_{ureA} with Mg (■), Ca (○), Mn(II) (△), or Ni(II) (●) in the titration buffer. The solid and dashed lines represent nonlinear least-squares fits to the 1:1 binding model, and K_d values of $5.7 \pm 0.21 \times 10^{-8}$, $5.0 \pm 2.6 \times 10^{-8}$, and $2.2 \pm 1.6 \times 10^{-8}$ M for Mg, Ca, and Mn(II), respectively, were determined. All FA experiments were performed in 20 mM Hepes, 100 mM NaCl, and 20 mM glycine at 25 °C.

addition of 250 μM Mg, and the anisotropy reached a plateau at approximately 3 mM Mg.

Ni-HPNikR−P_{ureA}-F Binding in the Presence of Other Divalent Metal Ions. To determine if magnesium was specifically required for [Ni-*HP*NikR]$_4$−P_{ureA} binding or if other divalent metal ions would also facilitate this binding interaction, FA studies with alternate divalent metal ions, Zn(II), Co(II), Ni(II), Ca(II), and Mn(II), were conducted. The studies revealed that in addition to Mg(II), Ca(II) and Mn(II) also facilitate DNA binding, whereas Zn(II), Co(II), and Ni(II) failed to do so. Additionally, titrations with monovalent potassium did not induce binding. Figure 5 shows the titration of P_{ureA}-*F* with [Ni-*HP*NikR]$_4$ in the presence of 3 mM $MgCl_2$, $CaCl_2$, $MnCl_2$, or $NiSO_4$ (as a representative of a nonbinding metal ion). A fit of the calcium and manganese data to a 1:1 binding equilibrium yielded dissociation constants: $K_d = 5.0 \pm 0.26 \times 10^{-8}$ and $2.2 \pm 0.16 \times 10^{-8}$ M, respectively. The titration with $NiSO_4$ did not result in any anisotropy changes and instead resulted in sample precipitation beyond the addition of 600 nM [Ni-*HP*NikR]$_4$.

Cu(II)-HPNikR−P_{ureA}-F Binding. Copper(II) can also bind to *HP*NikR at the high-affinity site (Figures S4 and S5); therefore, the affinity of [Cu(II)-*HP*NikR]$_4$ for P_{ureA}-*F* was probed using FA. As with Ni-*HP*NikR, a specific second metal ion, Mg, Ca, or Mn(II), was required for binding. Titrations of P_{ureA}-*F* with Cu(II)-*HP*NikR in the presence of magnesium, calcium, or manganese resulted in the following dissociation constants: $4.1 \pm 0.29 \times 10^{-8}$, $4.9 \pm 0.42 \times 10^{-8}$, and $8.1 \pm 1.0 \times 10^{-9}$ M, respectively. Table 2 compares these dissociation constants to those for the [Ni-(II)-*HP*NikR]$_4$−P_{ureA}-*F* complex.

Table 2: Dissociation Constants for [M-*HP*NikR]$_4$ [M = Ni(II) or Cu(II)] with P_{ureA}-*F* (K_d values in nanomolar)

low-affinity metal	[Ni(II)-*HP*NikR]$_4$	[Cu(II)-*HP*NikR]$_4$
Mg	57 ± 2.1	41 ± 2.9
Ca	50 ± 2.6	49 ± 4.2
Mn	22 ± 1.6	8.1 ± 1.0

DISCUSSION

*HP*NikR belongs to an emerging family of prokaryotic transcription factors that combine a ribbon−helix−helix DNA binding motif with a pre-ordered metal binding domain to regulate genes in response to metal ion occupancy (*14*). Unlike its homologues in other bacteria such as *E. coli* where the protein functions as a transcriptional *repressor* of a single gene, *HP*NikR functions as both a transcriptional *repressor* and transcriptional *activator* of multiple genes (*13*). The complete repertoire of genes that are *directly* regulated by *HP*NikR are not known, although gel shift analysis and DNase footprinting studies have identified seven genes that are directly regulated by *HP*NikR (*27*−*30*, *43*). The relative affinities of *HP*NikR for these genes' promoters have not been determined, and the relationship between the type of metal ions bound to *HP*NikR and the protein's preference for specific sequences is not fully understood. The goal of this study was to develop a solution-based assay to systematically probe the interactions between *HP*NikR and various gene promoter sequences.

Upon purification of apo-*HP*NikR, titrations with both Ni-(II) and Cu(II) were carried out to confirm that the protein, as isolated in our laboratory, bound these metal ions stoichiometrically. Intrinsic tryptophan fluorescence and CD studies were then performed to assess the effect of nickel ion coordination on the secondary and tertiary protein structure. The spectroscopic signature of apo-*HP*NikR using either assay did not change significantly when nickel was

bound, suggesting that nickel binding does not elicit global changes to the overall fold of the protein in solution. The recently reported series of X-ray structures of *HP*NikR in both the apo form and the partially nickel-bound form confirm that the presence of nickel does not result in a significant change in quaternary structure, although the fully nickel-bound form of *HP*NikR may require some change in quaternary structure (*20*).

To assess the effect of nickel on the overall protein stability, thermal denaturation studies were performed (Figure S1). Apo-*HP*NikR exhibits a single thermal melting transition with a midpoint of approximately 55 °C. The addition of nickel does not significantly perturb the unfolding transition midpoint, suggesting that nickel does little to stabilize the overall structure of the protein. In contrast, Zamble and coworkers have found that apo-*EC*NikR is stabilized by nickel; apo-*EC*NikR exhibits a biphasic unfolding curve when measured by thermal denaturation which becomes a single-step denaturation when nickel is added (*34*). The first unfolding transition for apo-*EC*NikR has been attributed to the C-terminal metal binding domain and the second to the N-terminal DNA binding domain (*18*, *34*). From our studies, the two domains of apo-*HP*NikR appear to unfold together, suggesting that the domains are more intimately associated than those of *EC*NikR.

A fluorescence anisotropy (FA) assay was developed to study the interaction between *HP*NikR and DNA. The promoter P_{ureA}, which corresponds to the regulatory region of the gene that encodes urease, was studied because it is a well-characterized example of a gene that is regulated by *HP*NikR in a nickel-dependent manner (*27*−*29*). Initial screening studies utilized P_{ureA}-*F*, a fluorescently labeled 49 bp double-stranded DNA oligonucleotide that spans a region of the *ureA* promoter identified by others using DNase footprinting studies as the binding site recognized by *HP*NikR (*27*−*29*). The DNA recognition sequence is proposed to be a 7 bp palindromic sequence linked by an 11 bp spacer (*28*). Titrations of P_{ureA} with either Ni(II)-*HP*NikR or Cu(II)-*HP*NikR under typical FA conditions (100 mM NaCl in buffer) did not exhibit any binding. It was necessary to add an additional, specific metal ion, magnesium, calcium, or manganese, to the buffer to at least 250 μM to observe binding. Addition of other divalent metal ions, including nickel(II), to the buffer did not promote binding. These findings suggest that *HP*NikR requires coordination of a second, specific low-affinity metal ion in addition to coordination of a high-affinity metal ion for function. Inspection of the sequence of *HP*NikR reveals that an additional nine amino acids are present at the N-terminus (M*D*TPNK*DD*S) of *HP*NikR that are absent in NikR homologues from other bacteria. Of particular interest are the three acidic aspartate residues (underlined) which we suggest may serve as binding ligands for this second, low-affinity metal ion. Aspartate is considered a "hard" base (or ligand) and will preferentially bind to a hard acid (or metal). The three divalent metal ions that promote DNA binding of *HP*NikR, magnesium, calcium, and manganese are all considered hard acids (or metals), whereas the divalent metal ions that do not promote DNA binding, nickel, copper, cobalt, and zinc, are all considered "borderline" acids and are less likely to bind to a hard base (*44*). Therefore, a Lewis acid−Lewis base interaction between specific hard acids and specific hard bases may play a role in the metal ion binding preferences of *HP*NikR's low-affinity site. It should be noted that the binding model for this low-affinity site is likely more complex than just a Lewis acid−Lewis base interaction and may involve other, yet to be identified, ligands from HPNikR and/or P_{ureA}.

*EC*NikR also contains a second low-affinity metal binding site; however, occupation of this second site is not absolutely required for DNA binding (*15*, *18*, *22*). Moreover, nickel and potassium have been shown to be the likely metals for the second site in *EC*NikR (*15*, *18*, *22*, *23*). Similarly, *Pyrococcus horikoshii* NikR (*PH*NikR) contains a second low-affinity metal binding site. Here nickel has been identified as the likely metal, and phosphate, as a mimic of DNA, has been shown to interact at this site, suggesting that nickel coordination may enhance DNA binding (*45*). Nickel or potassium does not promote binding between *HP*NikR and P_{ureA}, indicating that *HP*NikR and *EC*NikR/*PH*NikR have different metal requirements for their low-affinity sites and suggesting that the identity or location of these metal binding sites on each protein may differ.

The total cellular concentrations of magnesium, calcium, and manganese are not known for *H. pylori*; however, in *E. coli*, the total cellular concentration of magnesium is estimated to be >10 mM, that of calcium ~0.1 mM, and that of manganese in the micromolar range (*46*, *47*). If we assume that *H. pylori* houses at least similar concentrations of these metal ions, if not more due to liberation of metal ions from ingested foods in the gastric epithelium (*11*, *12*), magnesium is the most likely metal ion to occupy this proposed second site in *HP*NikR followed by calcium and manganese under physiological conditions.

The role of divalent metal ions in influencing the DNA binding properties of transcription factors has been well-documented; for example, the cAMP response element binding protein (CREB) requires magnesium for sequence-specific DNA binding by preventing nonspecific electrostatic interactions between CREB and nonconsensus DNA sequences (*48*, *49*), while both magnesium and calcium have been shown to regulate the DNA binding properties of DREAM, an EF-hand calcium binding protein (*50*). It would be of interest to determine whether magnesium has a similar role in dictating *HP*NikR sequence specificity with respect to the other identified *HP*NikR targets, i.e., the *nixA*, *hpn*, *fur*, and *nikR/exbB* divergent operators.

Full titrations of both Ni-*HP*NikR and Cu-*HP*NikR with P_{ureA}-*F* in the presence of magnesium, calcium, or manganese led to binding curves that could be fit to 1:1 binding equilibria. Ni(II)-*HP*NikR and Cu(II)-*HP*NikR bound P_{ureA}-*F* with affinities of 57 ± 2.1 and 41 ± 2.9 nM, with magnesium, 50 ± 2.6 and 49 ± 4.2 nM with calcium, and 22 ± 1.6 and 8.1 ± 1.0 nM with manganese, respectively. Both Ni(II)- and Cu(II)-substituted *HP*NikR exhibit similar trends in binding affinities as a function of the second metal ion, suggesting that both are functionally active; however, it must be noted that there was an absence of NikR-regulated genes identified in a recent RNA profiling study measuring the effect of copper ions on global gene regulation in *H. pylori* (*51*), suggesting that nickel is the physiologically functional metal. The affinity of Ni-*HP*NikR for P_{ureA} derived from analysis of a DNase footprinting experiment with a 196 bp DNA probe has been reported to be 50 ± 10 nM (*27*)

which closely matches the affinity of 57 ± 2.1 nM determined from our FA assay. Of note is that the DNAse footprinting studies were run with both magnesium and calcium in the buffer.

A competitive FA assay to probe the effect of DNA sequence on binding affinity was developed. A competitive titration with the P_{ureA} sequence exhibited a binding affinity similar to that of the direct titration with P_{ureA}-*F*, indicating that the fluorescent probe was not interfering with DNA binding. In contrast, a competitive titration with an altered DNA sequence in which the putative recognition palindrome had been removed exhibited no binding to Ni-*HP*NikR, providing evidence that the palindrome region is important for Ni-*HP*NikR recognition. Our success in developing a competitive FA assay sets the stage for future studies aimed at evaluating the sequence-specific requirements of *HP*-NikR−DNA recognition.

We have developed a FA assay that allows us to probe *HP*NikR−DNA binding as a function of metal ion coordination and DNA sequence. Using the P_{ureA} sequence as the DNA sequence, we have demonstrated that both forward and competitive FA titrations can be used to quantify the affinity of *HP*NikR for DNA. Our studies have revealed that for *HP*NikR to bind to P_{ureA}, a square planar metal ion [Ni(II) or Cu(II)] must be coordinated to the high-affinity metal binding site and a divalent, hard metal ion [Mg(II), Ca(II), or Mn(II)] must be coordinated to an as yet unidentified low-affinity site. As both magnesium and calcium are present in bacterial cells at concentrations sufficient to populate the low-affinity site under normal physiology, we propose that coordination of nickel to the high-affinity nickel site serves as the "switch" that initiates P_{ureA} binding and the subsequent transcription of urease. This model is consistent with the observations that nickel availability in *H. pylori* controls urease expression levels (*40*, *52*) and the observation that removal of the import of magnesium into *H. pylori* does not affect urease transcription (*53*). Current studies in our laboratory are focused on identifying the low-affinity metal binding site for *HP*NikR and on applying our FA assay to study other promoters regulated by *HP*NikR to understand how this protein can regulate multiple genes.

ACKNOWLEDGMENT

We thank Professor Peter Chivers at Washington University (St. Louis, MO) for providing us with unpublished DNA binding results for *HP*NikR and for useful discussions, Dr. Alisa Davis at the University of Zurich (Zurich, Switzerland) for help with data modeling in Mathematica, and Dr. Robert diTargiani at the University of Maryland for useful discussions.

SUPPORTING INFORMATION AVAILABLE

Apo-*HP*NikR and Ni-*HP*NikR thermal denaturation studies, Ni(II)-*HP*NikR and Cu(II)-*HP*NikR UV−visible spectra, and titration data. This material is available free of charge via the Internet at http://pubs.acs.org.

REFERENCES

1. Marshall, B. J., and Warren, J. R. (1984) Unidentified curved bacilli in the stomach of patients with gastritis and peptic ulceration, *Lancet 1*, 1311−1315.
2. Cover, T. L., and Blaser, M. J. (1992) *Helicobacter pylori* and gastroduodenal disease, *Annu. Rev. Med. 43*, 135−145.
3. Sepulveda, A. R., and Coelho, L. G. (2002) *Helicobacter pylori* and gastric malignancies, *Helicobacter 7* (Suppl. 1), 37−42.
4. Kusters, J. G., van Vliet, A. H., and Kuipers, E. J. (2006) Pathogenesis of *Helicobacter pylori* infection, *Clin. Microbiol. Rev. 19*, 449−490.
5. Loughlin, M. F. (2003) Novel therapeutic targets in *Helicobacter pylori*, *Expert Opin. Ther. Targets 7*, 725−735.
6. van Vliet, A. H., Kuipers, E. J., Stoof, J., Poppelaars, S. W., and Kusters, J. G. (2004) Acid-responsive gene induction of ammonia-producing enzymes in *Helicobacter pylori* is mediated via a metal-responsive repressor cascade, *Infect. Immun. 72*, 766−773.
7. Bik, E. M., Eckburg, P. B., Gill, S. R., Nelson, K. E., Purdom, E. A., Francois, F., Perez-Perez, G., Blaser, M. J., and Relman, D. A. (2006) Molecular analysis of the bacterial microbiota in the human stomach, *Proc. Natl. Acad. Sci. U.S.A. 103*, 732−737.
8. Bauerfeind, P., Garner, R., Dunn, B. E., and Mobley, H. L. (1997) Synthesis and activity of *Helicobacter pylori* urease and catalase at low pH, *Gut 40*, 25−30.
9. Maroney, M. J. (1999) Structure/function relationships in nickel metallobiochemistry, *Curr. Opin. Chem. Biol. 3*, 188−199.
10. Mulrooney, S. B., and Hausinger, R. P. (2003) Nickel uptake and utilization by microorganisms, *FEMS Microbiol. Rev. 27*, 239−261.
11. Bury-Mone, S., Thiberge, J. M., Contreras, M., Maitournam, A., Labigne, A., and De Reuse, H. (2004) Responsiveness to acidity via metal ion regulators mediates virulence in the gastric pathogen *Helicobacter pylori*, *Mol. Microbiol. 53*, 623−638.
12. Krishnaswamy, R., and Wilson, D. B. (2000) Construction and characterization of an *Escherichia coli* strain genetically engineered for Ni(II) bioaccumulation, *Appl. Environ. Microbiol. 66*, 5383−5386.
13. Contreras, M., Thiberge, J. M., Mandrand-Berthelot, M. A., and Labigne, A. (2003) Characterization of the roles of NikR, a nickel-responsive pleiotropic autoregulator of *Helicobacter pylori*, *Mol. Microbiol. 49*, 947−963.
14. Dosanjh, N. S., and Michel, S. L. J. (2006) Microbial nickel metalloregulation: NikRs for nickel ions, *Curr. Opin. Chem. Biol. 10*, 123−130.
15. Chivers, P. T., and Sauer, R. T. (2000) Regulation of high affinity nickel uptake in bacteria. Ni^{2+}-dependent interaction of NikR with wild-type and mutant operator sites, *J. Biol. Chem. 275*, 19735−19741.
16. de Pina, K., Desjardin, V., Mandrand-Berthelot, M. A., Giordano, G., and Wu, L. F. (1999) Isolation and characterization of the nikR gene encoding a nickel-responsive regulator in *Escherichia coli*, *J. Bacteriol. 181*, 670−674.
17. Chivers, P. T., and Sauer, R. T. (1999) NikR is a ribbon-helix-helix DNA-binding protein, *Protein Sci. 8*, 2494−2500.
18. Chivers, P. T., and Sauer, R. T. (2002) NikR repressor: High-affinity nickel binding to the C-terminal domain regulates binding to operator DNA, *Chem. Biol. 9*, 1141−1148.
19. Schreiter, E. R., Sintchak, M. D., Guo, Y., Chivers, P. T., Sauer, R. T., and Drennan, C. L. (2003) Crystal structure of the nickel-responsive transcription factor NikR, *Nat. Struct. Biol. 10*, 794−799.
20. Dian, C., Schauer, K., Kapp, U., McSweeney, S. M., Labigne, A., and Terradot, L. (2006) Structural Basis of the Nickel Response in *Helicobacter pylori*: Crystal Structures of HpNikR in Apo and Nickel-bound States, *J. Mol. Biol. 361*, 715−730.
21. Carrington, P. E., Chivers, P. T., Al-Mjeni, F., Sauer, R. T., and Maroney, M. J. (2003) Nickel coordination is regulated by the DNA-bound state of NikR, *Nat. Struct. Biol. 10*, 126−130.
22. Bloom, S. L., and Zamble, D. B. (2004) Metal-selective DNA-binding response of *Escherichia coli* NikR, *Biochemistry 43*, 10029−10038.
23. Schreiter, E. R., Wang, S. C., Zamble, D. B., and Drennan, C. L. (2006) NikR-operator complex structure and the mechanism of repressor activation by metal ions, *Proc. Natl. Acad. Sci. U.S.A. 103*, 13676−13681.
24. Fauquant, C., Diederix, R. E., Rodrigue, A., Dian, C., Kapp, U., Terradot, L., Mandrand-Berthelot, M. A., and Michaud-Soret, I. (2006) pH dependent Ni(II) binding and aggregation of *Escherichia coli* and *Helicobacter pylori* NikR, *Biochimie 11*, 1693−1705.
25. van Vliet, A. H., Ernst, F. D., and Kusters, J. G. (2004) NikR-mediated regulation of *Helicobacter pylori* acid adaptation, *Trends Microbiol. 12*, 489−494.

26. Tomb, J. F., White, O., Kerlavage, A. R., Clayton, R. A., Sutton, G. G., Fleischmann, R. D., Ketchum, K. A., Klenk, H. P., Gill, S., Dougherty, B. A., Nelson, K., Quackenbush, J., Zhou, L., Kirkness, E. F., Peterson, S., Loftus, B., Richardson, D., Dodson, R., Khalak, H. G., Glodek, A., McKenney, K., Fitzegerald, L. M., Lee, N., Adams, M. D., Hickey, E. K., Berg, D. E., Gocayne, J. D., Utterback, T. R., Peterson, J. D., Kelley, J. M., Cotton, M. D., Weidman, J. M., Fujii, C., Bowman, C., Watthey, L., Wallin, E., Hayes, W. S., Borodovsky, M., Karp, P. D., Smith, H. O., Fraser, C. M., and Venter, J. C. (1997) The complete genome sequence of the gastric pathogen *Helicobacter pylori*, *Nature 388*, 539−547.
27. Abraham, L. O., Li, Y., and Zamble, D. B. (2006) The metal- and DNA-binding activities of *Helicobacter pylori* NikR, *J. Inorg. Biochem. 100*, 1005−1014.
28. Delany, I., Ieva, R., Soragni, A., Hilleringmann, M., Rappuoli, R., and Scarlato, V. (2005) In vitro analysis of protein-operator interactions of the NikR and fur metal-responsive regulators of coregulated genes in *Helicobacter pylori*, *J. Bacteriol. 187*, 7703−7715.
29. Ernst, F. D., Kuipers, E. J., Heijens, A., Sarwari, R., Stoof, J., Penn, C. W., Kusters, J. G., and van Vliet, A. H. (2005) The Nickel-Responsive Regulator NikR Controls Activation and Repression of Gene Transcription in *Helicobacter pylori*, *Infect. Immun. 73*, 7252−7258.
30. Ernst, F. D., Stoof, J., Horrevoets, W. M., Kuipers, E. J., Kusters, J. G., and van Vliet, A. H. (2006) NikR Mediates Nickel-Responsive Transcriptional Repression of the *Helicobacter pylori* Outer Membrane Proteins FecA3 (HP1400) and FrpB4 (HP1512), *Infect. Immun. 74*, 6821−6828.
31. Sreerama, N., and Woody, R. W. (2000) Estimation of protein secondary structure from circular dichroism spectra: Comparison of CONTIN, SELCON and CDSSTR methods with an expanded reference set, *Anal. Biochem. 287*, 252−260.
32. Gatto, G. J., Jr., Maynard, E. L., Guerrerio, A. L., Geisbrecht, B. V., Gould, S. J., and Berg, J. M. (2003) Correlating structure and affinity for PEX5:PTS1 complexes, *Biochemistry 42*, 1660−1666.
33. Lakowicz, J. R. (1999) *Principles of Fluorescence Spectroscopy*, pp 291−319, Kluwer Academic/Plenium Publishers, New York.
34. Wang, S. C., Dias, A. V., Bloom, S. L., and Zamble, D. B. (2004) Selectivity of metal binding and metal-induced stability of *Escherichia coli* NikR, *Biochemistry 43*, 10018−10028.
35. Pain, R. (1996) Determining the CD spectrum of a protein, in *Current Protocols in Protein Science* (Coligan, J. E., Hidde, L., Ploegh, B. M. D., Speicher, D. W., Wingfield, P. T., and Taylor, S. E. G., Eds.) pp 7.6.1−7.6.23, John Wiley & Sons Inc., New York.
36. Wang, Y., Hemmingsen, L., and Giedroc, D. P. (2005) Structural and functional characterization of *Mycobacterium tuberculosis* CmtR, a PbII/CdII-sensing SmtB/ArsR metalloregulatory repressor, *Biochemistry 44*, 8976−8988.
37. Golynskiy, M. V., Davis, T. C., Helmann, J. D., and Cohen, S. M. (2005) Metal-induced structural organization and stabilization of the metalloregulatory protein MntR, *Biochemistry 44*, 3380−3389.
38. Zheleznova, E. E., Crosa, J. H., and Brennan, R. G. (2000) Characterization of the DNA- and metal-binding properties of *Vibrio anguillarum* fur reveals conservation of a structural Zn^{2+} ion, *J. Bacteriol. 182*, 6264−6267.
39. Eaton, K. A., Brooks, C. L., Morgan, D. R., and Krakowka, S. (1991) Essential role of urease in pathogenesis of gastritis induced by *Helicobacter pylori* in gnotobiotic piglets, *Infect. Immun. 59*, 2470−2475.
40. van Vliet, A. H., Poppelaars, S. W., Davies, B. J., Stoof, J., Bereswill, S., Kist, M., Penn, C. W., Kuipers, E. J., and Kusters, J. G. (2002) NikR mediates nickel-responsive transcriptional induction of urease expression in *Helicobacter pylori*, *Infect. Immun. 70*, 2846−2852.
41. Jantz, D., and Berg, J. M. (2004) Reduction in DNA-binding affinity of Cys_2His_2 zinc finger proteins by linker phosphorylation, *Proc. Natl. Acad. Sci. U.S.A. 101*, 7589−7593.
42. Lieser, S. A., Davis, T. C., Helmann, J. D., and Cohen, S. M. (2003) DNA-binding and oligomerization studies of the manganese(II) metalloregulatory protein MntR from *Bacillus subtilis*, *Biochemistry 42*, 12634−12642.
43. Davis, G. S., Flannery, E. L., and Mobley, H. L. (2006) *Helicobacter pylori* HP1512 Is a Nickel-Responsive NikR-Regulated Outer Membrane Protein, *Infect. Immun. 74*, 6811−6820.
44. Lippard, S. J., and Berg, J. M. (1994) *Principles of Bioinorganic Chemistry*, University Science Books, Mill Valley, CA.
45. Chivers, P. T., and Tahirov, T. H. (2005) Structure of *Pyrococcus horikoshii* NikR: Nickel sensing and implications for the regulation of DNA recognition, *J. Mol. Biol. 348*, 597−607.
46. Outten, C. E., and O'Halloran, T. V. (2001) Femtomolar sensitivity of metalloregulatory proteins controlling zinc homeostasis, *Science 292*, 2488−2492.
47. Finney, L. A., and O'Halloran, T. V. (2003) Transition metal speciation in the cell: Insights from the chemistry of metal ion receptors, *Science 300*, 931−936.
48. Craig, J. C., Schumacher, M. A., Mansoor, S. E., Farrens, D. L., Brennan, R. G., and Goodman, R. H. (2001) Consensus and variant cAMP-regulated enhancers have distinct CREB-binding properties, *J. Biol. Chem. 276*, 11719−11728.
49. Moll, J. R., Acharya, A., Gal, J., Mir, A. A., and Vinson, C. (2002) Magnesium is required for specific DNA binding of the CREB B-ZIP domain, *Nucleic Acids Res. 30*, 1240−1246.
50. Osawa, M., Dace, A., Tong, K. I., Valiveti, A., Ikura, M., and Ames, J. B. (2005) Mg^{2+} and Ca^{2+} differentially regulate DNA binding and dimerization of DREAM, *J. Biol. Chem. 280*, 18008−18014.
51. Waidner, B., Melchers, K., Ivanov, I., Loferer, H., Bensch, K. W., Kist, M., and Bereswill, S. (2002) Identification by RNA profiling and mutational analysis of the novel copper resistance determinants CrdA (HP1326), CrdB (HP1327) and CzcB (HP1328) in *Helicobacter pylori*, *J. Bacteriol. 184*, 6700−6708.
52. van Vliet, A. H., Kuipers, E. J., Waidner, B., Davies, B. J., de Vries, N., Penn, C. W., Vandenbroucke-Grauls, C. M., Kist, M., Bereswill, S., and Kusters, J. G. (2001) Nickel-responsive induction of urease expression in *Helicobacter pylori* is mediated at the transcriptional level, *Infect. Immun. 69*, 4891−4897.
53. Pfeiffer, J., Guhl, J., Waidner, B., Kist, M., and Bereswill, S. (2002) Magnesium uptake by CorA is essential for viability of the gastric pathogen *Helicobacter pylori*, *Infect. Immun. 70*, 3930−3934.

BI062092W